BMJ Open Respiratory Research

Fibrotic extracellular vesicles contribute to mechanical ventilation-induced pulmonary fibrosis development by activating lung fibroblasts via JNK signalling pathway: an experimental study

Ri Tang, Yang Zhou, Shuya Mei, Qiaoyi Xu, Jinhua Feng, Shunpeng Xing, Yuan Gao, Shaojie Qin, Zhengyu He

Abstract Recent research has revealed that mechanical ventilation (MV) could initiate ventilator-induced lung injury along with the initiation of the process of pulmonary fibrosis (PF), leading to MV-induced PF (MVPF). However, the underlying mechanism remains unclear. This study aimed to explore the role of MV-induced extracellular vesicles (MV-EVs) and the c-Jun N-terminal kinase (JNK) signalling pathway in the pathogenesis of MVPF in vivo and in vitro. The process of MV is accompanied by the secretion of MV-EVs, which could induce lung fibroblast activation. Furthermore, single-cell RNA-sequencing analysis revealed that the JNK pathway in lung fibroblasts was activated after MV initiation. Inhibiting the JNK pathway could both restrain MV-EV-induced lung fibroblast activation in vitro or reduce the severity of MVPF in vivo. In conclusion, this study demonstrated that MV-EVs contribute to MVPF progression by activating lung fibroblasts via the JNK signalling pathway and that inhibiting the secretion of EV and the activation of the JNK signalling pathway is a promising strategy for treating MVPF.

WHAT IS ALREADY KNOWN ON THIS TOPIC

⇒ Mechanical ventilation (MV) is an effective treatment for patients with respiratory failure. However, MV can also lead to MV-induced pulmonary fibrosis (MVPF). The precise molecular and cellular pathways contributing to the development of MVPF remain poorly explored.

WHAT THIS STUDY ADDS

⇒ MV-induced extracellular vesicles (MV-EVs) contribute to the development of MVPF by activating lung fibroblasts via the c-Jun N-terminal kinase (JNK) signalling pathway.

HOW THIS STUDY MIGHT AFFECT RESEARCH, PRACTICE OR POLICY

⇒ The inhibition of EV release and the activation of the JNK signalling pathway may be a window for molecular-targeted therapy for MVPF.

To cite: Tang R, Zhou Y, Mei S, *et al*. Fibrotic extracellular vesicles contribute to mechanical ventilation-induced pulmonary fibrosis development by activating lung fibroblasts via JNK signalling pathway: an experimental study. *BMJ Open Respir Res* 2023;**10**:e001753. doi:10.1136/bmjresp-2023-001753

RT and YZ contributed equally.

Received 11 April 2023
Accepted 31 July 2023

For numbered affiliations see end of article.

Correspondence to
Professor Zhengyu He;
zhengyuheshsmu@163.com
and

Shaojie Qin;
18018599869@163.com

INTRODUCTION

From scheduled surgical procedures to acute respiratory failure, mechanical ventilation (MV) is the most widely used short-term life support technique worldwide.[1] Patients with severe acute respiratory distress syndrome (ARDS) frequently require prolonged MV, with mean duration of approximately 12 days.[2] The complications of MV have received increasing attention because numerous clinical randomised controlled trials have been conducted.[1 3–8] An important complication of MV is MV-induced pulmonary fibrosis (MVPF). Experimental and clinical studies have found that MV, which is necessary for life support in patients with ARDS, could cause pulmonary fibrosis (PF).[2 9 10] Mortality and morbidity may be significantly affected by this factor.[2] In previous studies, it has been reported that the mechanism of MVPF is related to epithelial–mesenchymal transition,[11] signalling pathway activation[12 13] and metabolic reprogramming.[14] At present, in our clinical work, small tidal-volume MV strategy and allowable hypercapnia MV strategy were used to decrease the occurrence of MVPF. The precise molecular and cellular pathways contributing to MVPF remain poorly explored. This highlights the need for further research to elucidate the mechanisms involved.

As a result of fibroblast proliferation and extracellular matrix (ECM) remodelling, PF leads to respiratory insufficiency.[15] Lung fibroblasts are the key main effector cells of PF. Excessive ECM secreted by lung fibroblasts

and its deposition may reduce pulmonary compliance and stiffen tissue, hence affecting lung function.[16 17] Fibronectin and α-smooth muscle actin (α-SMA) are the major characterised components of the ECM.[18 19] The level of ECM secretion is reflected in the expression of these proteins.[20] In addition to the protein expression of the ECM, the ability of fibroblasts to proliferate and migrate is also considered a key character in pulmonary fibroblast activation.[21] Identifying the mechanism underlying fibroblast activation is crucial in preventing and treating PF.

Recent advances indicate a mechanistic link between extracellular vesicles (EVs) and PF.[22] EV components can be influenced by the physiological or pathological status of producing cells.[23] EVs from specific cell types such as senescent cells and activated immune cells can induce PF.[24] Multiple studies have shown the emerging roles of EV cargoes in the epithelial–mesenchymal trophic unit during the development of PF.[22] In our previous study, we demonstrate that ASK1-ER stress pathway-mediated fibrotic EV release from alveolar epithelial cells contributes to fibroblast activation and the onset of PF during MV.[25] However, the exact mechanisms responsible for inducing MVPF with EVs remain unclear. We investigated the effect of MV-EVs (EV extracted from the bronchoalveolar lavage fluid (BALF) of the MV group) in inducing lung fibroblast activation. Our single-cell RNA-sequencing analysis indicated that MVPF was associated with the activation of the c-Jun N-terminal kinase (JNK) signalling pathway in lung fibroblasts. The contribution of the JNK signalling pathway to PF has been well investigated.[26–28] By regulating lung inflammation and fibroblast viability, differentiation and migration, the JNK pathways could directly promote the development of bleomycin (BLM)-induced PF.[29] What is more, JNK signalling pathways mediate interleukin (IL)-33 to induce the production of cytokines transforming growth factor-β, IL-13, tumour necrosis fator-α and IL-6,[30] which could induce fibrosis process. The role of MV-induced EVs (MV-EVs) in mediating JNK signalling pathway activation involved in MVPF is unclear.

In this study, we constructed the MV-treated mice model of MVPF and MV-EV-treated lung fibroblast cellular model, using EV secretion and JNK pathway inhibitors to demonstrate the role of MV-EVs and the JNK signalling pathway in the pathogenesis of MVPF in vivo and in vitro.

MATERIALS AND METHODS

Animals

We obtained C57BL/6 male mice (6–8 weeks; 18–28 g) from Shanghai SLAC Laboratory Animals (China). There was no specific pathogen present in the housing environment, and the temperature was controlled (22–24°C), a 12-hour light/dark cycle was observed, and food and water were freely available to the animals.

Patient and public involvement

Patients and the public were not involved in this study's design, recruitment and conduct.

Cell lines and culture

We obtained the human lung fibroblast MRC-5 cell line from the Cell Bank of the Chinese Academy of Sciences (China). MRC-5 cells were cultured in Dulbecco's Minimum Essential Medium from Gibco, USA, with 10% fetal bovine serum (FBS) from Gibco (USA), 100 IU/mL penicillin and streptomycin from Gibco. EV was removed from all FBS used for cell culture by ultracentrifugation at 100 000 g for 70 min.

Reagents and antibodies

The JNK signalling pathway inhibitor SP600125 (S1460) was purchased from Selleck (USA). The EV secretion inhibitor GW4869 (S7609) was purchased from Selleck (USA). The primary antibodies used in this study were rabbit anti-fibronectin (ab2413, Abcam, USA), mouse anti-α-SMA (ab5694, Abcam, USA), rabbit anti-p-JNK (#4668, CST, USA), rabbit anti-JNK (#9252, CST, USA), mouse anti-β-actin (#3700, CST, USA) and mouse anti-α-tubulin (#3873 CST, China). In addition, goat anti-mouse (#7076, CST, USA) and goat anti-rabbit (#7074, CST, USA) were used as secondary antibodies.

Experimental grouping and design of the mice

The mice were anaesthetised with ketamine (200 mg/kg) and xylazine (10 mg/kg) intraperitoneally. To establish the MVPF model, the mice were treated with MV for 2 hours with the following parameters: fractional inspired oxygen, 0.21; tidal volume, 20 mL/kg; and respiratory rate, 70 breaths/min.[31] JNK inhibitor SP600125 and EV secretion inhibitor GW4869 were injected intraperitoneally before MV. On day 7 following MV, mice were euthanized with an overdose of euthanized to collect lungs, blood and BALF.

GW4869 (2.5 mg/kg in corn oil), an EV secretion inhibitor, was administered via intraperitoneal injection once a day for 3 consecutive days before MV.[32] Mice were randomly assigned into sham (n=6), GW4869 (n=6), MV (n=6) and MV+GW4869 (n=6). Mice in the MV and MV+GW4869 groups received MV treatment for 2 hours.

SP600125 (15 mg/kg in corn oil), a JNK inhibitor, was administered via intraperitoneal injection once a day for 3 consecutive days before intubation.[33] Mice were randomly assigned into sham (n=6), SP600125 (n=6), MV (n=6) and MV+SP600125 (n=6). Mice in the MV and MV+SP600125 groups received MV treatment for 2 hours.

Experimental grouping and design of MRC-5 cells

In 6-well culture plates, MRC-5 cells were plated at a density of 2×10^4 per well. To starve the cells overnight, the medium was changed to serum-free minimum essential medium once the cells had adhered and reached

70% confluency. Then, the cells were incubated with BALF-EVs (MV-EVs or NC-EVs, 50 µg EVs protein/sample). An inhibitor of the JNK pathway, SP600125, was used to suppress JNK activity. Twenty-four hours after treatment, the cells and supernatants were collected.

Confluent MRC-5 cells were randomly assigned into the sham, SP600125, MV-EV and MV-EV+SP600125 groups. MRC-5 cells in the sham group received phosphate-buffered saline (PBS) treatment as a control; MRC-5 cells in the SP600125 group were cultured in a medium containing 20 µM SP600125 for 2 hours; MRC-5 cells in the MV-EV group received MV-EVs (50 µg EVs protein/sample) for 24 hours; and MRC-5 cells in the MV-EV+SP600125 group were cultured in a medium containing 20 µM SP600125 for 2 hours and received MV-EVs (50 µg EVs protein/sample) for 24 hours.

EV isolation, characterisation and labelling

BALFs were sequentially centrifuged one at 500 g, one at 2500 g and one at 12 000 g, and the supernatant was collected. A pellet was isolated and resuspended in 20 µL PBS for later use after being centrifuged at 100 000 g for 70 min.

Transmission electron microscope (TEM) was used to visualise the pellet after adsorption for 90 s onto a copper mesh coated with carbon. Uranyl acetate dye solution was used for the negative staining test for 30 s. Using a NanoSight NS300 instrument (Malvern Panalytica, UK), nanoparticle tracking analysis (NTA) was used to measure the diameter of the pellet. Western blotting (WB) was used to detect the surface marker proteins of the pellet. EVs were labelled with PKH-67 membrane dye (MIDI67, Sigma-Aldrich, USA) according to the manufacturer's instructions.

Single-cell RNA-sequencing analysis

We used single-cell RNA sequencing to analyse mouse lung cells. Gene expression data have been deposited into the SRA database at the National Center for Biotechnology Information with accession number SUB11878630. A single-cell RNA sequence was used to analyse mice pulmonary cells from the MV and sham groups. The number and viability of prepared single cells were measured using the Rigel S2 (Countstar, China). Using the Chromium Single Cell 3' V2 Chemistry Library Kit and Gel Bead & Multiplex Kit from 10x Genomics (Biomarker Technologies, China), single-cell libraries were constructed. Gel Bead-In-Emulsions were generated using cellular suspensions loaded onto the Chromium Controller (10x Genomics, Pleasanton). The Chromium Single Cell 3' Reagent Kits V.3.1 (10x Genomics) were used to generate bar-coded sequencing libraries. Each sample was sequenced using paired-end sequencing on one lane of NovaSeq 6000 with 150 nt each end after library preparation. The 10x Genomics Cell Ranger pipeline was used to process raw reads. With Cell Ranger, the single cells can be clustered, the marker genes can be identified and the unique molecular identifiers can be exported. The R package Seurat (V.2.2) was used for further analysis. For most of the Seurat analyses, default parameters were used. The maximum cut-off for Feature Plot was 0.5.

Pulmonary histopathology

For collagen identification, the left lung was fixed in 4% paraformaldehyde (PFA) and stained with Masson's trichrome. The Ashcroft fibrosis score was used to quantify PF.[34] During the histological examination of the lungs, a pathologist blinded to the experimental groups performed the examination. In this study, pulmonary injury was graded on a scale of 0–4 (0, normal; 1, light; 2, moderate; 3, strong; 4, intense) using the following nine reference parameters: microscopic emphysema, perivascular haemorrhage, alveolar oedema, perivascular oedema, congestion, microscopic atelectasis, alveolar haemorrhage, alveolar and interstitial polymorphonuclear leucocyte infiltration, and hyaline membrane formation.[35]

Immunofluorescence staining

Formalin-fixed, paraffin-embedded sections of pulmonary tissue or cultured cells fixed with 4% PFA and permeabilised with 0.25% Triton X100 were stained with appropriate primary antibodies. Anti-mouse IgG (H+L), F(ab')2 Fragment (Alexa Fluor 488 Conjugate) (#4408, CST, USA), anti-mouse IgG (H+L), F(ab')2 Fragment (Alexa Fluor 594 Conjugate) (#8890, CST, USA), anti-rabbit IgG (H+L), F(ab')2 Fragment (Alexa Fluor 488 Conjugate) (#4412, CST, USA) and anti-rabbit IgG (H+L), F(ab')2 Fragment (Alexa Fluor 594 Conjugate) (#8889, CST, USA) were used as secondary antibodies. Cell nuclei were stained using 4',6-diamidino-2-phenylindole (Santa Cruz Biotechnology, Heidelberg, Germany).

Cell viability assay (Cell Counting Kit-8 assay)

MRC-5 cells were cultured in 96-well plates. The Cell Counting Kit-8 (CCK-8) assay (Vazyme, China) was used to evaluate the viability of MRC-5 cells according to the manufacturer's instructions. Briefly, after adding CCK-8 solution to each well, MRC-5 cells were incubated for 2 hours. The optical density of each well was measured using a DNM-9602 enzyme-labelled analyser (Beijing Perlong New Technology Co).

Cell proliferation assay (EDU assay)

MRC-5 cells were cultured in 6-well plates. The EDU Alexa Fluor 594 imaging kit (Epizyme, China) was used to evaluate MRC-5 cell proliferation according to the manufacturer's instructions.

Briefly, after adding EDU solution to each well, the MRC-5 cells were incubated for 2 hours. Incubated MRC-5 cells were fixed in 75% ethyl alcohol for 24 hours at 20°C and penetrated with 0.3% PBS with Tween (PBST) for

30 min. Three washings in 0.1% PBST for 15 min were followed by 30 min incubation in EDU click solution (with Alexa Fluor 594) away from light.

Wound healing migration assay

MRC-5 cells were cultured in 6-well plates. The plates were scratched using a 200 µL pipette tip led by a scratch ruler after the MRC-5 cells were cultured to 80% confluence. An inverted light microscope (magnification: ×100, Olympus, Japan) was used to capture images of each same place 0 and 24 hours after treatment and cultivation.

Western blotting

We separated proteins using sodium dodecyl sulfate-polyacrylamide gel electrophoresis and transferred them to polyvinylidene difluoride membranes. The membranes were incubated with primary and secondary antibodies. Enhanced ECL Chemiluminescent Substrate Kit (Vazyme, China) was used to detect blots using Image Lab (Bio-Rad, USA).

Statistical analysis

We display the data as means±SEM. Multiple comparisons with group and time factors were performed using a two-way analysis of variance, followed by the Bonferroni test. For the in vitro experiments, a non-parametric test was performed to compare cells with and without stretch. GraphPad Prism V.5.0 (GraphPad Software, La Jolla, California, USA) was used for all analyses, and p values of <0.05 were used to denote statistical significance.

RESULTS

MV initiated the process of PF

To create the MVPF model in vivo, mice were observed 7 days after MV at 20 mL/kg for 2 hours. Histologically, pulmonary injury, interstitial leucocyte infiltration, alveolar oedema and haemorrhage were more obvious in the MV group than in the sham group. Masson staining displayed an increase in collagen deposition in the pulmonary interstitium after MV. The total pulmonary injury and fibrosis scores were increased in the MV group (figure 1A).

Consistent with the histological observations, MV significantly increased the protein levels of fibronectin and α-SMA in the lungs (figure 1B). MV was also associated with an upregulation of fibronectin+/collagen I+ in total cells, compared with the sham group (figure 1C).

Inhibition of EV secretion alleviates the severity of MVPF

Studies revealed that EVs were associated with organ fibrosis. We isolated and purified EVs from BALF. TEM and NTA determined the structure and size of the particles isolated from BALF. The BALF-EV markers CD63 was detected using WB (figure 2A). To investigate whether the inhibition of EV release in vivo affects MVPF development and progression, mice were intraperitoneally pretreated with GW4869 (EV secretion inhibitor). As shown in figure 2B, the severity of pulmonary histopathology could be attenuated by GW4869 pretreatment.

Immunofluorescence staining showed that MV significantly increased the percentage of fibronectin+ and α-SMA+ in total cells (figure 2C), whereas WB showed upregulated protein levels of fibronectin and α-SMA in pulmonary tissue (figure 2D). Furthermore, these responses could be alleviated by pretreating with GW4869 (figure 2B–D). Therefore, we speculated that inhibiting EV secretion contributes to the alleviation of MVPF.

MV-EVs induce lung fibroblast activation

To investigate the role of EVs, we next used MRC-5 cells (human lung fibroblasts) as the target cells to evaluate the functions of NC-EVs (EVs attracted from BALF in the sham group) and MV-EVs (EVs attracted from BALF in the MV group). After treating MRC-5 cells with PKH-67-labelled EVs (green) (50 µg EVs protein/sample), figure 3A shows that the EVs were taken up by MRC-5 cells.

To further elucidate the effects of EVs on MRC-5 cells, the differentiation, proliferation and migration abilities of MRC-5 cells were measured. Using the CCK-8 and EDU assays, our data showed that when MRC-5 cells took up MV-EVs, the cell viability and proliferation ability were increased compared with those of the MRC-5 cells that took up NC-EV or the sham group (figure 3B,D), indicating that MV-EVs increased the proliferation ability of MRC-5 cells. Similarly, using a wound healing assay, our data showed that the cell migration ability was increased when the MRC-5 cells took up MV-EVs compared with that in the MRC-5 cells that took up NC-EV or the sham group (figure 3C). The WB and immunofluorescence staining were both performed to evaluate the expression of differentiation-related proteins. Fibronectin and α-SMA were chosen to reflect the ECM secretion and the differentiation level. Our data showed that after treatment with MV-EVs, the expression of differentiation-related proteins was increased in MRC-5 cells, whereas the NC-EVs and sham groups did not exert significant changes (figure 3E,F). Our findings showed that MV-EVs induced lung fibroblast activation.

Single-cell RNA-sequencing analysis revealed that the JNK pathway is involved in the fibrosis process after MV in fibroblast cluster

To detect the mechanism of fibroblast differentiation, we performed single-cell RNA sequencing to analyse pulmonary cells from mice from the sham and MV groups. Raw reads were processed using a 10x Genomics Cell Ranger pipeline. With Cell Ranger, the single cells can be clustered, and the marker genes can be identified. The UMAP plot was used to display all cell types (figure 4A). As the core effector cells of PF, fibroblast cluster marker genes are shown in figure 4B.

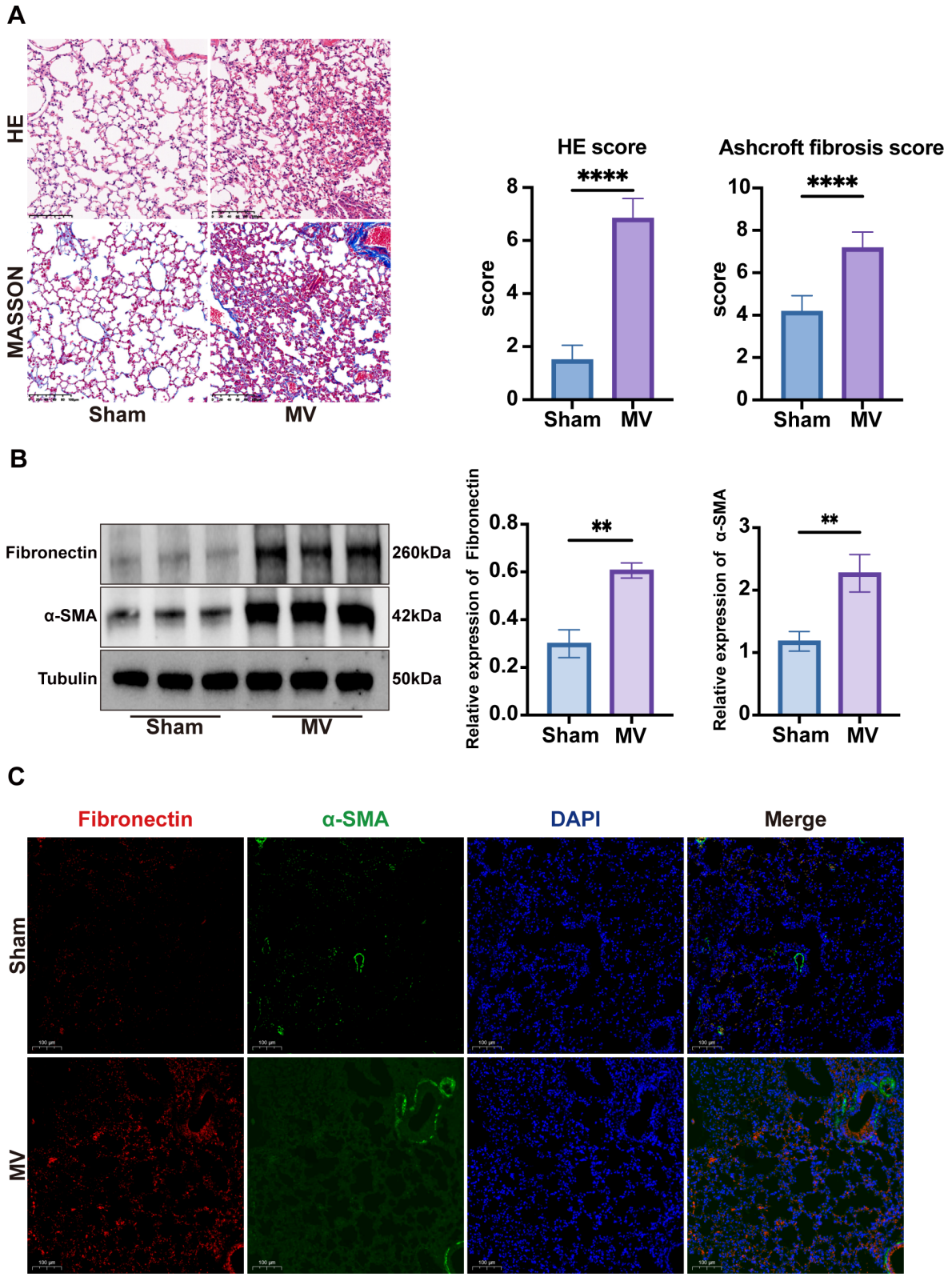

Figure 1 Mechanical ventilation (MV) initiated the process of pulmonary fibrosis. (A) Lung injury was assessed by H&E staining. Collagen deposition was assessed with Masson staining and evaluated through the Ashcroft fibrosis score. Original magnification ×200. Scale bars correspond to 100 µm (n=6). (B) Fibrosis was quantified by determining the protein levels of fibronectin and α-smooth muscle actin (α-SMA) in lung tissues via western blotting. Relative densitometry of the protein bands of fibronectin and α-SMA over tubulin is displayed in bar graphs (n=6). (C) Lung tissues were stained with fluorophore-labelled antibodies against fibronectin (Alexa Fluor 594, red) and α-SMA (Alexa Fluor 488, green). The 4',6-diamidino-2-phenylindole (DAPI) stain was used to detect nuclei (blue). Original magnification ×200. Scale bars correspond to 100 µm (n=6). Data are expressed as means±SEM. *p<0.05, **p<0.01, ***p<0.001, ****p<0.0001.

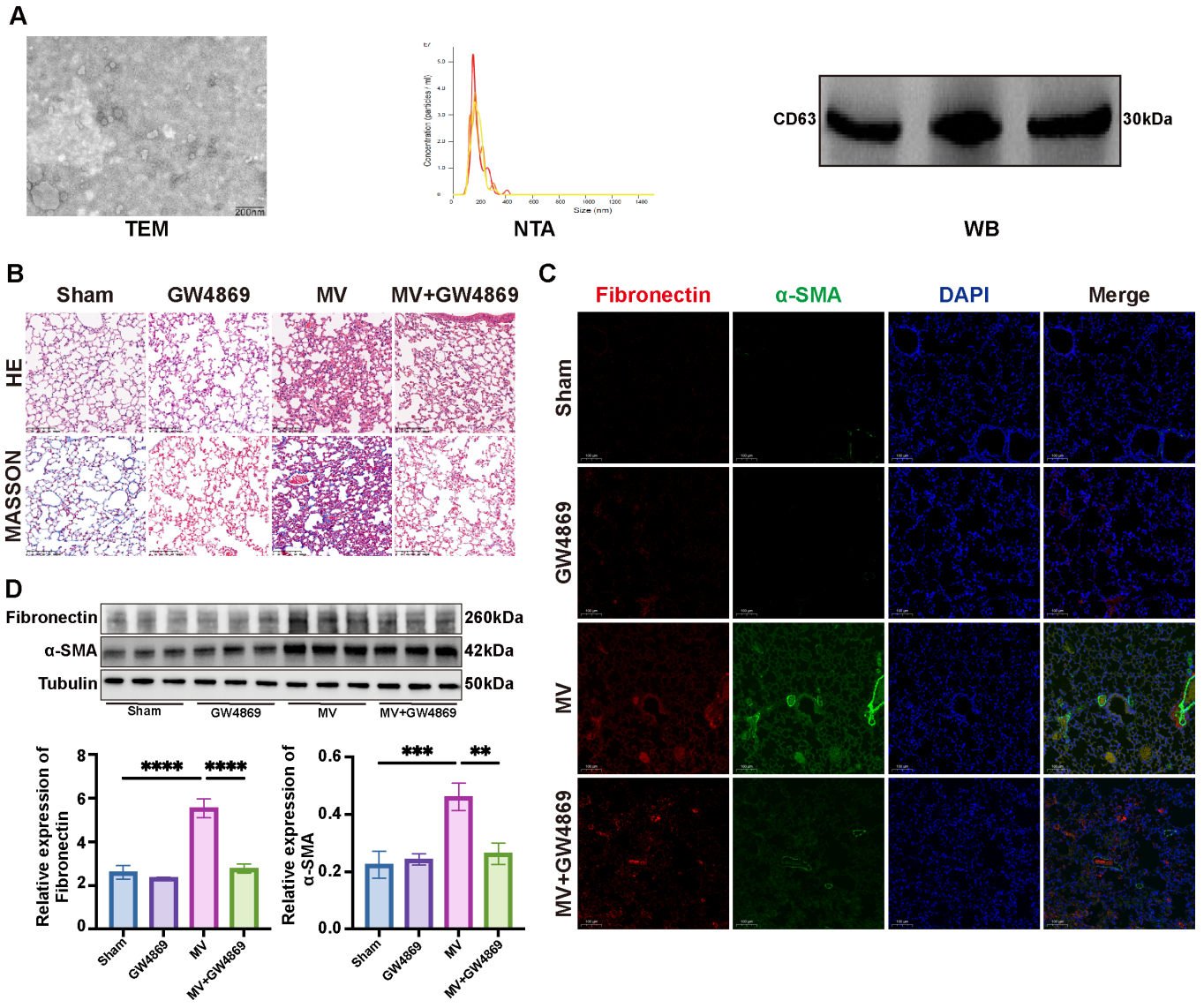

Figure 2 Inhibition of extracellular vesicle (EV) secretion alleviates the severity of mechanical ventilation (MV)-induced pulmonary fibrosis. (A) EVs were quantified using TEM, NTA and WB. (B) Lung injury was assessed with H&E staining. Collagen deposition was assessed with Masson staining. Original magnification ×200. Scale bars correspond to 100 µm (n=6). (C) Lung tissues were stained with fluorophore-labelled antibodies against fibronectin (Alexa Fluor 594, red) and α-SMA (Alexa Fluor 488, green). The 4',6-diamidino-2-phenylindole (DAPI) stain was used to detect nuclei (blue). Original magnification ×200. Scale bars correspond to 100 µm (n=6). (D) Fibrosis was quantified by determining the protein levels of fibronectin and α-SMA in lung tissues via WB. Relative densitometry of the protein bands of fibronectin and α-SMA over tubulin is displayed in bar graphs (n=6). Data are expressed as means±SEM. *P<0.05, **p<0.01, ***p<0.001, ****p<0.0001. α-SMA, α-smooth muscle actin; NTA, nanoparticle tracking analysis; TEM, transmission electron microscope; WB, western blotting.

With the FindMarkers R packages, differentially expressed genes (DEGs) of the fibroblast clusters between the sham and MV groups were detected. By Gene Ontology enrichment analysis of DEGs in fibroblasts, we found significantly changed processes associated with fibrosis, such as 'ECM' and 'focal adhesion' (figure 4C). By Kyoto Encyclopedia of Genes and Genomes (KEGG) enrichment analysis of DEGs in fibroblasts, we found that the mitogen-activated protein kinase (MAPK) pathway might be a possible mechanism involved in fibroblast activation (figure 4D). The mammalian MAPK family consists of extracellular signal-regulated kinase (ERK), p38 and JNK (also known as stress-activated protein kinase).[36] According to the results of the Gene Set Enrichment Analysis (figure 4E), we speculated that the JNK pathway is involved in the fibrosis process after MV in fibroblast cluster.

Inhibition of the JNK pathway inhibits MV-EV-induced lung fibroblast activation

According to our analysis of our single-cell data, we sought to demonstrate whether JNK pathway activation was involved in MV-EV-induced MRC-5 cell activation.

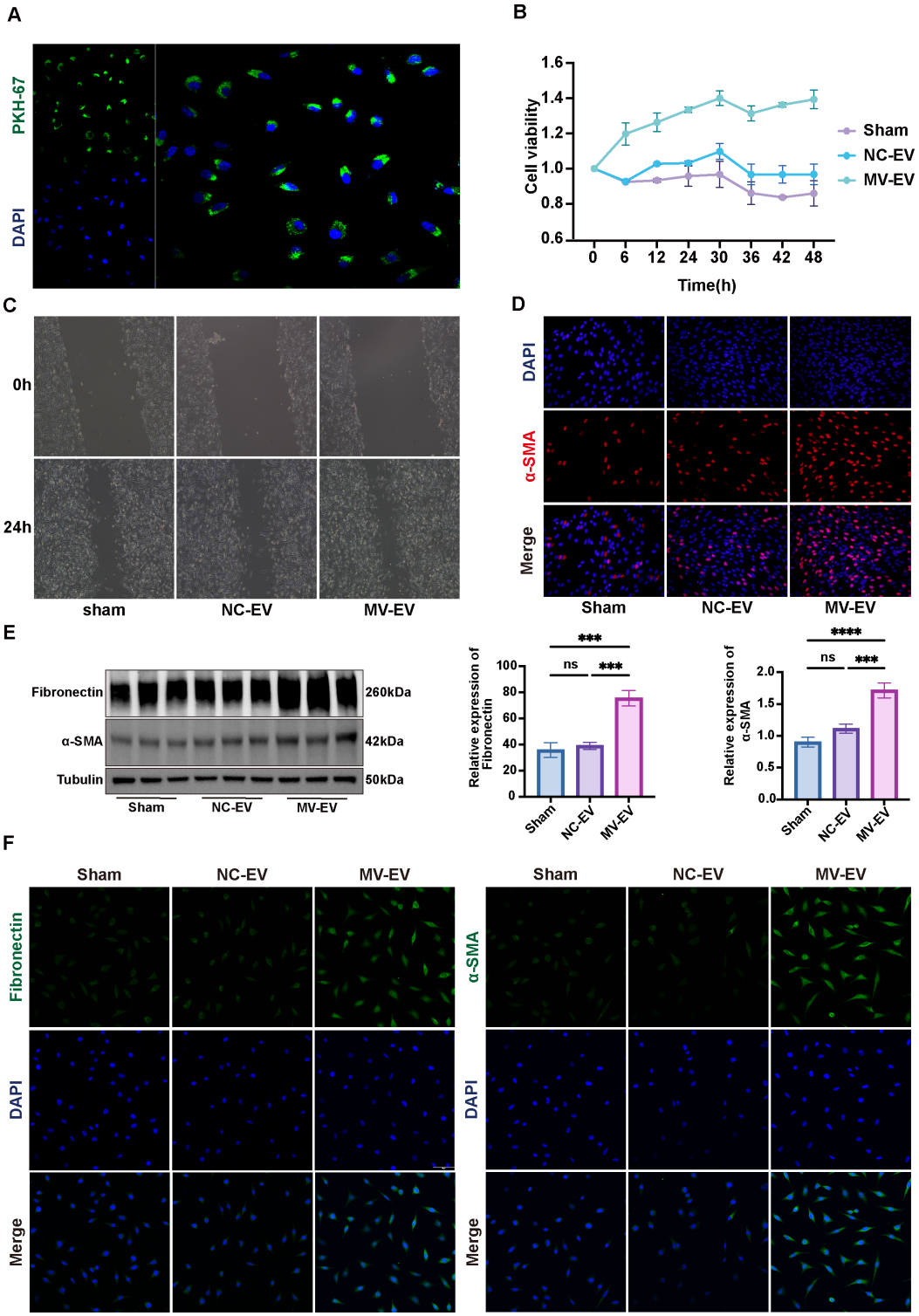

Figure 3 MV-EVs induce lung fibroblast activation. (A) Confocal microscopy shows fluorescence of the uptake of PKH-67-labelled EVs (Alexa Fluor 488, green) in MRC-5 cells. Original magnification ×400. Scale bars correspond to 50 µm (n=3). (B) CCK-8 assay was performed to evaluate the viability of MRC-5 cells by different groups (n=3). (C) Wound healing assay was performed to evaluate the migration ability of MRC-5 cells by different groups (n=3). (D) EDU assay was performed to evaluate the proliferation ability of MRC-5 cells by different groups (n=3). (E) Fibrosis was quantified by determining the protein levels of fibronectin and α-SMA in lung tissues via WB. Relative densitometry of the protein bands of fibronectin and α-SMA over tubulin is displayed in bar graphs (n=3). (F) MRC-5 cells were stained with fluorophore-labelled antibodies against fibronectin and α-SMA (Alexa Fluor 488, green). The 4',6-diamidino-2-phenylindole (DAPI) stain was used to detect nuclei (blue). Original magnification ×800. Scale bars correspond to 20 µm (n=3). Data are expressed as means±SEM. *P<0.05, **p<0.01, ***p<0.001, ****p<0.0001. α-SMA, α-smooth muscle actin; CCK-8, Cell Counting Kit-8; MV-EVs, mechanical ventilation-induced extracellular vesicles; ns, not significant; WB, western blotting.

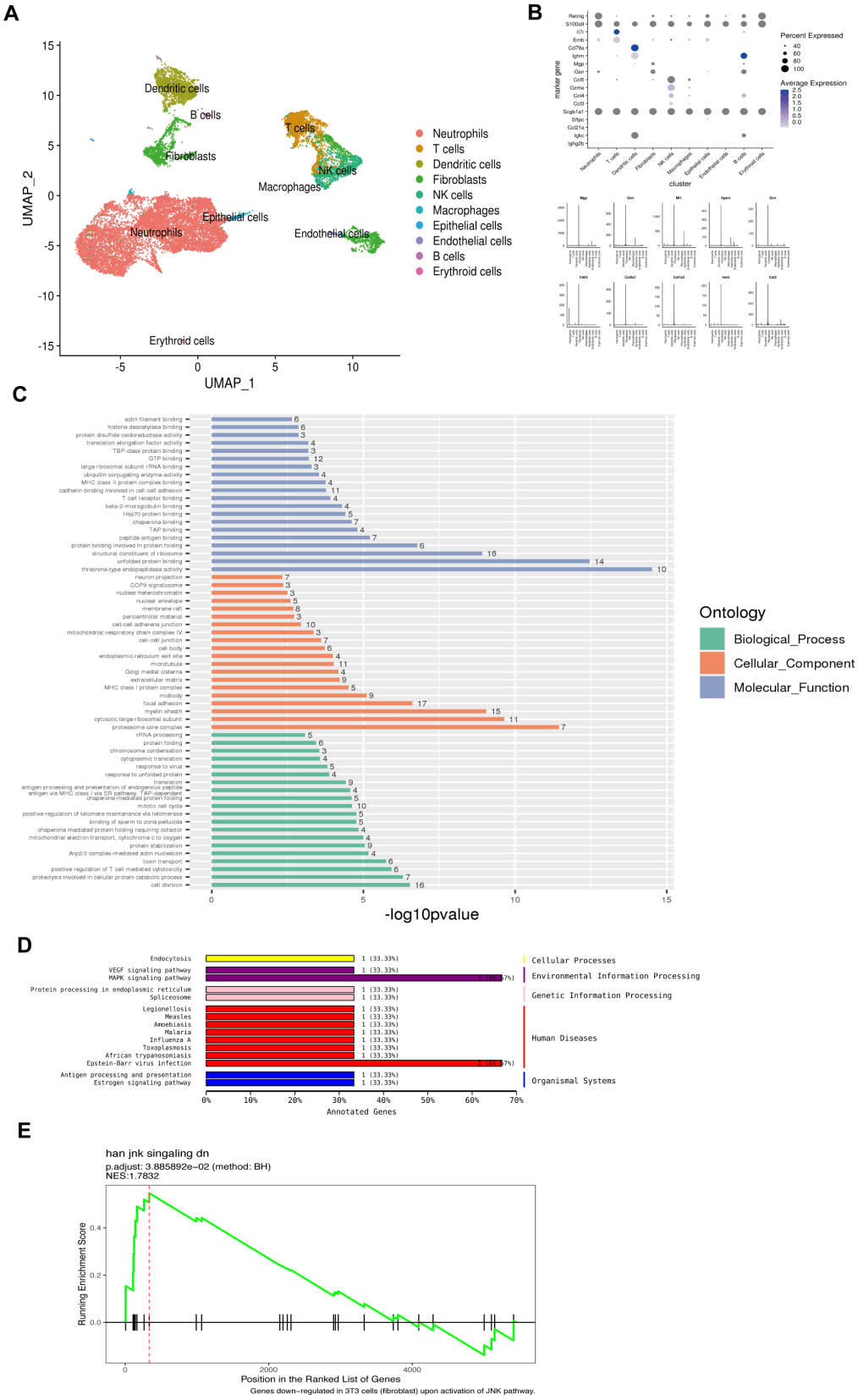

Figure 4 Single-cell RNA-sequencing analysis reveals that the JNK pathway is involved in the fibrosis process after MV in fibroblast cluster. (A) The UMAP plot of all cell types. (B) Cluster marker genes of fibroblasts. (C) GO enrichment analysis with DEGs of fibroblast clusters between the sham and MV groups. (D) KEGG enrichment analysis of DEGs of fibroblast clusters between the sham and MV groups. (E) GSEA of fibroblast clusters between the sham and MV groups. DEGs, differentially expressed genes; GO, Gene Ontology; GSEA, Gene Set Enrichment Analysis; JNK, c-Jun N-terminal kinase; KEGG, Kyoto Encyclopedia of Genes and Genomes; MV, mechanical ventilation.

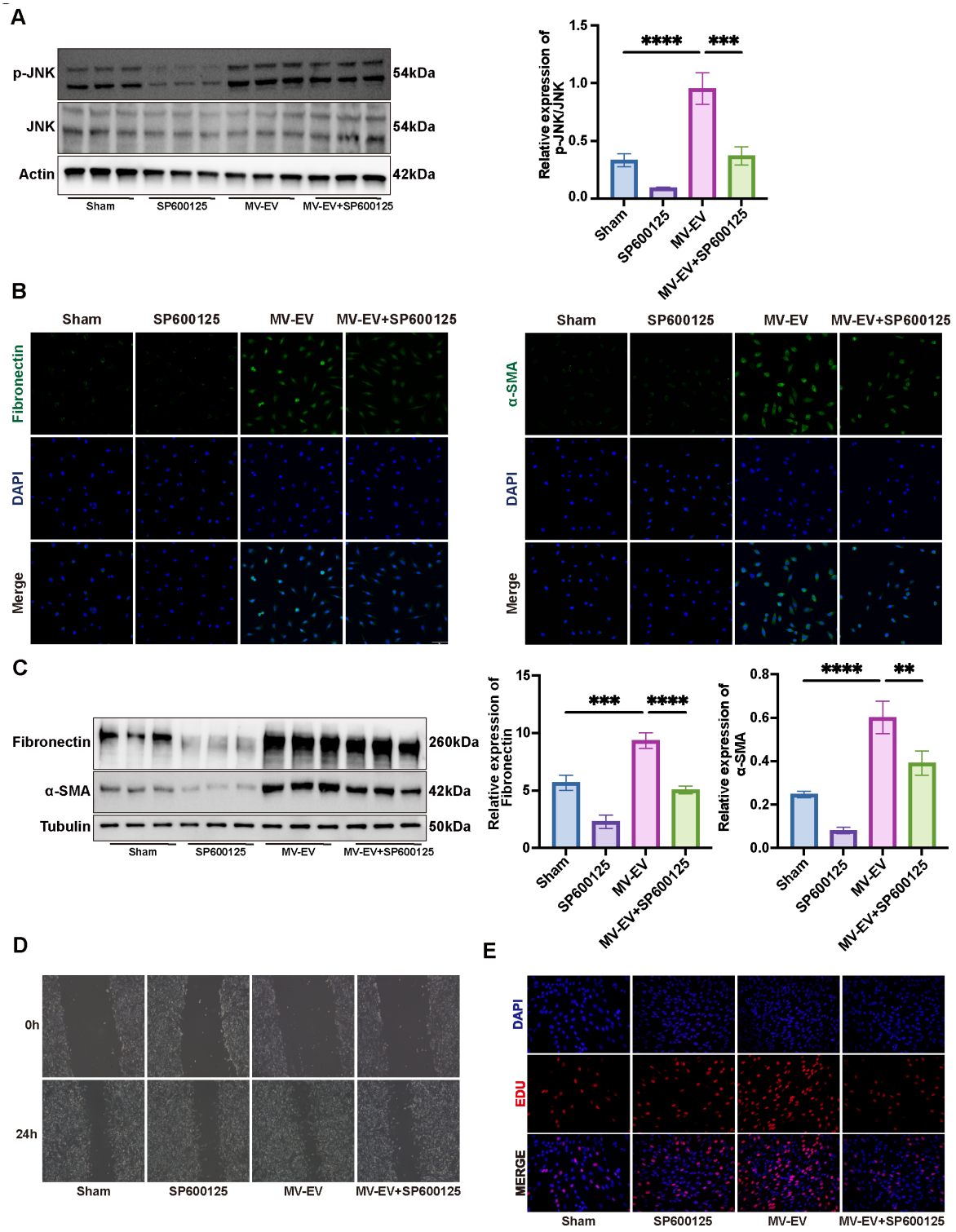

Figure 5 Inhibition of the JNK pathway reduces MV-EV-induced lung fibroblast activation. (A) The protein expression of JNK and p-JNK in MRC-5 cells was determined via WB. Relative densitometry of the protein bands of p-JNK over JNK is displayed in bar graphs (n=3). (B) MRC-5 cells were stained with fluorophore-labelled antibodies against fibronectin and α-SMA (Alexa Fluor 488, green). The 4',6-diamidino-2-phenylindole stain (DAPI) was used to detect nuclei (blue). Original magnification ×800. Scale bars correspond to 20 µm (n=3). (C) Fibrosis was also quantified by determining the protein levels of fibronectin and α-SMA in lung tissues via WB. Relative densitometry of the protein bands of fibronectin and α-SMA over tubulin is displayed in bar graphs (n=3). (D) Wound healing assay was performed to evaluate the migration ability of MRC-5 cells by different groups (n=3). (E) EDU assay was performed to evaluate the proliferation ability of MRC-5 cells by different groups (n=3). Data are expressed as means±SEM. *P<0.05, **p<0.01, ***p<0.001, ****p<0.0001. α-SMA, α-smooth muscle actin; JNK, c-Jun N-terminal kinase; MV-EV, mechanical ventilation-induced extracellular vesicle; p-JNK, phosphorylated JNK; WB, western blotting.

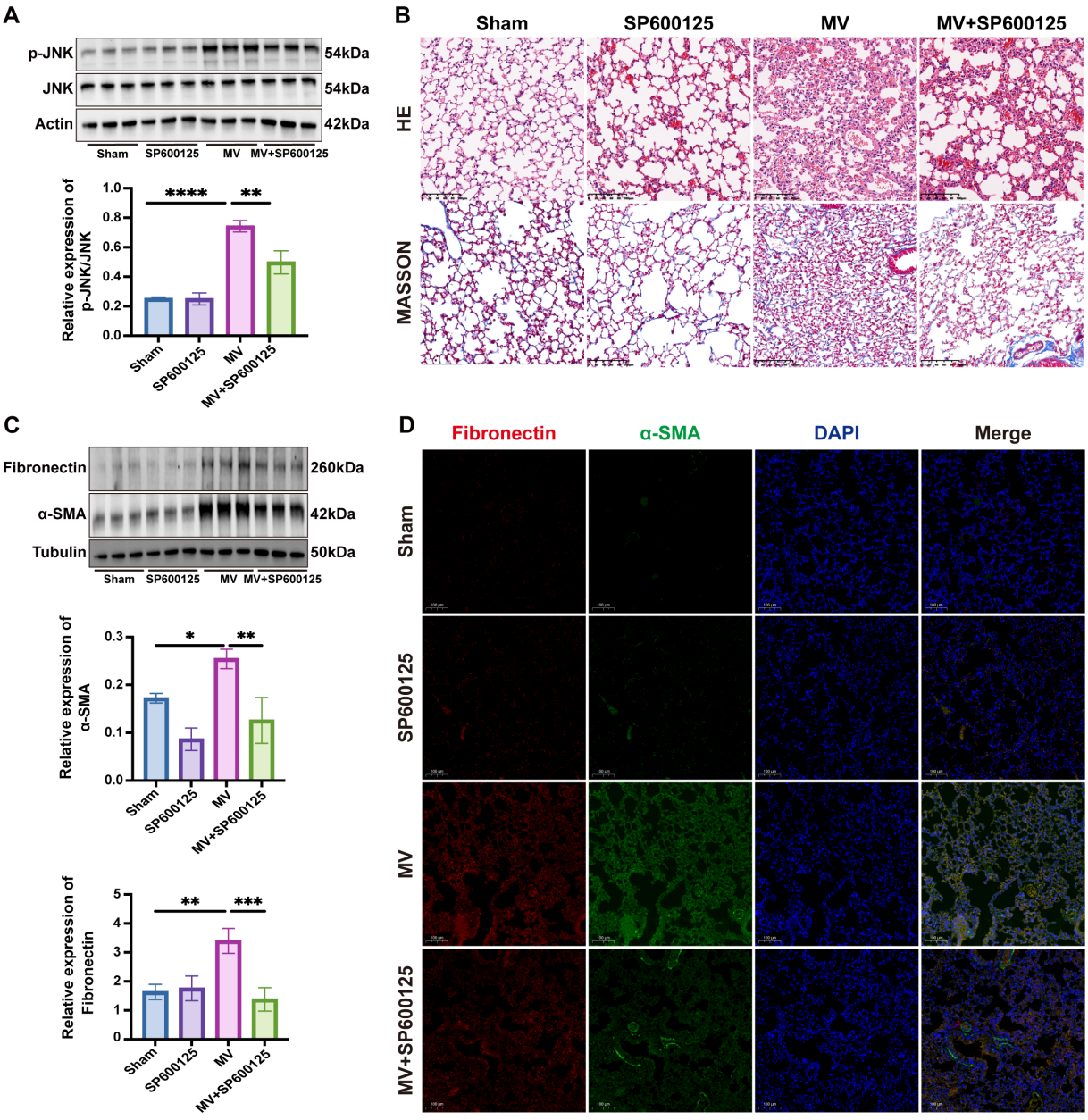

Figure 6 Inhibition of the JNK pathway reduces the severity of MVPF. (A) The protein expression of JNK and p-JNK was determined via WB. Relative densitometry of the protein bands of p-JNK over JNK is displayed in bar graphs (n=6) (B) .Lung injury was assessed with H&E staining. Collagen deposition was assessed with Masson staining. Original magnification ×200. Scale bars correspond to 100 µm (n=6). (C) Fibrosis was also quantified by determining the protein levels of fibronectin and α-SMA in lung tissues via WB. Relative densitometry of the protein bands of fibronectin and α-SMA over tubulin is displayed in bar graphs (n=6). (D) Lung tissues were stained with fluorophore-labelled antibodies against fibronectin (Alexa Fluor 594, red) and α-SMA (Alexa Fluor 488, green). The 4',6-diamidino-2-phenylindole (DAPI) stain was used to detect nuclei (blue). Original magnification ×200. Scale bars correspond to 100 µm (n=6). Data are expressed as means±SEM. *P<0.05, **p<0.01, ***p<0.001, ****p<0.0001. α-SMA, α-smooth muscle actin; JNK, c-Jun N-terminal kinase; MV, mechanical ventilation; MVPF, MV-induced pulmonary fibrosis; p-JNK, phosphorylated JNK; WB, western blottin.

As shown in figure 5A, WB indicated that the protein level of JNK was not changed, whereas the protein level of phosphorylated JNK (p-JNK) was upregulated in MRC-5 cells after treatment with MV-EVs.

Because SP600125 could suppress the JNK pathway, we explored whether suppressing the JNK pathway affects the activation of MRC-5 cells. WB and immunofluorescence staining demonstrated that MV-EVs increased the differentiation ability in MRC-5 cells, which could be suppressed by pretreating with SP600125 (figure 5B,C). Using the wound healing assay, our data showed that the cell migration ability was increased when MRC-5 cells took up MV-EVs; these processes could be suppressed by pretreating with SP600125 (figure 5D). Similarly, using the EDU assay, figure 5E shows that by pretreating with SP600125 before taking up MV-EVs in MRC-5 cells, the

increased proliferation ability in the MV-EV group would be suppressed. Therefore, it is reasonable to imply that the inhibition of the JNK pathway could reduce MV-EV-induced lung fibroblast activation.

Inhibition of the JNK pathway alleviated the severity of MVPF

To elucidate the effects of a JNK inhibitor in vivo, mice with MVPF were used to observe the effects of SP600125. The mice were injected intraperitoneally with 15 mg/kg concentrations of SP600125 before MV. After 7 days of MV, lung tissue samples from these mice were separated for WB, histopathology and immunofluorescence staining.

As shown in figure 6A, the increased protein level of p-JNK/JNK could be decreased in the SP600125-treated group compared with that in the MV group. Through H&E and Masson staining, our data showed that pulmonary histopathology could be decreased in the MV+SP600125 group compared with that in the MV group (figure 6B). Immunofluorescence and WB were performed to show the expression of fibronectin and α-SMA in pulmonary tissue. Our data showed that both fibronectin and α-SMA were reduced in the MV+SP600125 group compared with those in the MV group (figure 6C,D). Certainly, SP600125-treated mice without MV did not show obvious differences from those in the sham group. Our findings showed that SP600125 reduced the expression of fibrosis-related genes and histopathology changes in mice treated with MV, indicating that the inhibition of the JNK pathway reduced the severity of MVPF.

DISCUSSION

MV is an effective treatment for patients with respiratory failure. However, MV can also lead to ventilator-induced lung injury, MVPF and other adverse effects. Papazian *et al*[37] reported that 53% of patients with ARDS treated with MV for 5 days or longer had PF. In a prospective cohort study of 25 consecutive mechanically ventilated patients with ARDS, Martin *et al*[38] reported that the mortality rate of patients with lung fibrosis was 57% (8 of 14 patients), whereas the mortality rate in patients without fibrosis was 0%. However, the mechanisms underlying MVPF remain unclear. In this study, we found that the MV-EVs-JNK signalling pathway plays an essential role in increasing the differentiation, proliferation and migration of lung fibroblasts, which aggravated the process of MVPF after MV.

Recent attention has been drawn to the effects of EVs as shuttles for crucial cargo and their involvement in coordinating and disseminating information about homeostasis and disease. Relevant research revealed that EVs were associated with PF regardless of whether the focus was on therapy[39] or pathogenesis.[40] However, the role of EVs in MVPF has attracted less attention. In our study, we confirmed that PF could be decreased after MV by inhibiting EVs secreted by GW4869. In the next step, we confirmed that MV-EV could induce lung fibroblast activation. Finally, we believe that MV-EVs could be involved in regulating MVPF by activating lung fibroblasts.

To detect the mechanism of fibroblast activation in MVPF, we analysed the DEGs of fibroblasts in our single-cell RNA-sequence data. The KEGG enrichment analysis revealed that the MAPK signalling pathway in fibroblasts was highly altered after MV. Numerous biological processes, including inflammation and fibrosis responses, are regulated by the signalling pathways of MAPKs (these MAPKs consist of three members: ERK, JNK and p38).[41–44] According to a study focused on BLM-induced pulmonary fibrosis, the JNK signalling pathway regulates fibroblast viability, differentiation and migration, which directly promote the development of PF.[29 44] However, the relationship between the JNK signalling pathway and MVPF has not been fully investigated. In our study, we implied that by inhibiting the JNK signalling pathway with SP600125, the increased differentiation, migration and proliferation abilities of MV-EV-treated MRC-5 cells could be suppressed in vitro, and the degree of MVPF could be reduced in vivo.

A limitation of our study is that we did not examine the full content of MV-EVs. Therefore, whole transcriptomic sequencing of MV-EVs is planned to address this limitation.

CONCLUSION

In conclusion, this study demonstrated that MV-EVs contribute to MVPF development and progression by activating lung fibroblasts via the JNK signalling pathway. Inhibiting the secretion of EVs and activating the JNK signalling pathway are promising strategies for treating MVPF.

Author affiliations
Department of Critical Care Medicine, Ren Ji Hospital, Shanghai Jiao Tong University School of Medicine, Shanghai, China

Contributors RT, YZ, SQ and ZH supervised the study. RT and YZ performed the research. SM and QX participated in data collection and figure arrangement. JF and SX participated in data analysis and interpretation. YG, SQ and ZH were involved in the conception and design of the study. All authors read, commented on and approved the manuscript.

Funding This research was supported by grants from the National Natural Science Foundation of China (NSFC, no. 82172150), Renji Hospital Clinical Research Innovation and Cultivation Fund (RJPY-DZX-008) and the Shanghai Science and Technology Development Foundation (22YF1423300).

Competing interests None declared.

Patient and public involvement Patients and/or the public were not involved in the design, or conduct, or reporting, or dissemination plans of this research.

Patient consent for publication Not required.

Ethics approval Our experiments were approved by the Animal Care and Use Committee of Renji Hospital, Shanghai Jiaotong University School of Medicine (no. RJ2020-0625).

Provenance and peer review Not commissioned; externally peer reviewed.

Data availability statement Data are available in a public, open access repository.

ORCID iD
Zhengyu He http://orcid.org/0000-0001-7354-850X

REFERENCES

1 Pham T, Brochard LJ, Slutsky AS. Mechanical ventilation: state of the art. *Mayo Clin Proc* 2017;92:1382–400.
2 Cabrera-Benitez NE, Laffey JG, Parotto M, *et al*. Mechanical ventilation-associated lung fibrosis in acute respiratory distress syndrome: a significant contributor to poor outcome. *Anesthesiology* 2014;121:189–98.
3 Slutsky AS, Ranieri VM. Ventilator-induced lung injury. *N Engl J Med* 2013;369:2126–36.
4 Mathis MR, Duggal NM, Likosky DS, *et al*. Intraoperative mechanical ventilation and postoperative pulmonary complications after cardiac surgery. *Anesthesiology* 2019;131:1046–62.
5 Goligher EC, Dres M, Fan E, *et al*. Mechanical ventilation-induced diaphragm atrophy strongly impacts clinical outcomes. *Am J Respir Crit Care Med* 2018;197:204–13.
6 Slutsky AS. History of mechanical ventilation. from vesalius to ventilator-induced lung injury. *Am J Respir Crit Care Med* 2015;191:1106–15.
7 Baid H. Patient safety: identifying and managing complications of mechanical ventilation. *Crit Care Nurs Clin North Am* 2016;28:451–62.
8 McGuckin D. Mechanical ventilation mode and postoperative pulmonary complications. *Anaesthesia* 2018;73:252–3.
9 Fang X-Z, Li M, Wang Y-X, *et al*. Mechanosensitive ion channel Piezo1 mediates mechanical ventilation-exacerbated ARDS-associated pulmonary fibrosis. *J Adv Res* 2022.
10 Villar J, Cabrera-Benítez NE, Valladares F, *et al*. Tryptase is involved in the development of early ventilator-induced pulmonary fibrosis in sepsis-induced lung injury. *Crit Care* 2015;19:138.
11 Cabrera-Benítez NE, Parotto M, Post M, *et al*. Mechanical stress induces lung fibrosis by epithelial-mesenchymal transition. *Crit Care Med* 2012;40:510–7.
12 Zhang R, Pan Y, Fanelli V, *et al*. Mechanical stress and the induction of lung fibrosis via the midkine signaling pathway. *Am J Respir Crit Care Med* 2015;192:315–23.
13 Liao HD, Mao Y, Ying YG. The involvement of the laminin-integrin A7B1 signaling pathway in mechanical ventilation-induced pulmonary fibrosis. *J Thorac Dis* 2017;9:3961–72.
14 Mei S, Xu Q, Hu Y, *et al*. Integrin B3-Pkm2 pathway-mediated aerobic glycolysis contributes to mechanical ventilation-induced pulmonary fibrosis. *Theranostics* 2022;12:6057–68.
15 Hsu H-S, Liu C-C, Lin J-H, *et al*. Involvement of ER stress, Pi3K/AKT activation, and lung fibroblast proliferation in Bleomycin-induced pulmonary fibrosis. *Sci Rep* 2017;7:14272.
16 Ma Z-G, Yuan Y-P, Wu H-M, *et al*. Cardiac fibrosis: new insights into the pathogenesis. *Int J Biol Sci* 2018;14:1645–57.
17 Fan Z, Xu Z, Niu H, *et al*. Spatiotemporal delivery of basic fibroblast growth factor to directly and simultaneously attenuate cardiac fibrosis and promote cardiac tissue vascularization following myocardial infarction. *J Control Release* 2019;311–312:233–44.
18 Shinde AV, Humeres C, Frangogiannis NG. The role of A-smooth muscle actin in fibroblast-mediated matrix contraction and remodeling. *Biochim Biophys Acta Mol Basis Dis* 2017;1863:298–309.
19 Singh P, Carraher C, Schwarzbauer JE. Assembly of fibronectin extracellular matrix. *Annu Rev Cell Dev Biol* 2010;26:397–419.
20 Jhala D, Rather H, Kedaria D, *et al*. Biomimetic polycaprolactone-chitosan nanofibrous substrate influenced cell cycle and ECM secretion affect cellular uptake of nanoclusters. *Bioact Mater* 2019;4:79–86.
21 Deng Z, Fear MW, Suk Choi Y, *et al*. The extracellular matrix and mechanotransduction in pulmonary fibrosis. *Int J Biochem Cell Biol* 2020;126:105802.
22 Fujita Y. Extracellular vesicles in idiopathic pulmonary fibrosis: pathogenesis and therapeutics. *Inflamm Regen* 2022;42:23.
23 de Jong OG, Verhaar MC, Chen Y, *et al*. Cellular stress conditions are reflected in the protein and RNA content of endothelial cell-derived exosomes. *J Extracell Vesicles* 2012;1.
24 Kadota T, Fujita Y, Yoshioka Y, *et al*. Emerging role of extracellular vesicles as a senescence-associated secretory phenotype: insights into the pathophysiology of lung diseases. *Mol Aspects Med* 2018;60:92–103.
25 Tang R, Mei S, Xu Q, *et al*. Ask1-ER stress pathway-mediated fibrotic-EV release contributes to the interaction of alveolar epithelial cells and lung fibroblasts to promote mechanical ventilation-induced pulmonary fibrosis. *Exp Mol Med* 2022;54:2162–74.
26 Xiong Y, Cui X, Zhou Y, *et al*. Dehydrocostus lactone inhibits BLM-induced pulmonary fibrosis and inflammation in mice via the JNK and P38 MAPK-mediated NF-KB signaling pathways. *Int Immunopharmacol* 2021;98:107780.
27 Ji Y, Dou Y-N, Zhao Q-W, *et al*. Paeoniflorin suppresses TGF-B mediated epithelial-mesenchymal transition in pulmonary fibrosis through a smad-dependent pathway. *Acta Pharmacol Sin* 2016;37:794–804.
28 Wang J, He F, Chen L, *et al*. Resveratrol inhibits pulmonary fibrosis by regulating miR-21 through MAPK/AP-1 pathways. *Biomed Pharmacother* 2018;105:37–44.
29 Yang J-Y, Tao L-J, Liu B, *et al*. Wedelolactone attenuates pulmonary fibrosis partly through activating AMPK and regulating RAF-Mapks signaling pathway. *Front Pharmacol* 2019;10:151.
30 Göpfert C, Andreas N, Weber F, *et al*. The P38-Mk2/3 Module is critical for IL-33-induced signaling and cytokine production in dendritic cells. *J Immunol* 2018;200:1198–206.
31 Lv Z, Wang Y, Liu Y-J, *et al*. Nlrp3 Inflammasome activation contributes to mechanical stretch-induced endothelial-mesenchymal transition and pulmonary fibrosis. *Crit Care Med* 2018;46:e49–58.
32 Qin X, Lin X, Liu L, *et al*. Macrophage-derived exosomes mediate silica-induced pulmonary fibrosis by activating fibroblast in an endoplasmic reticulum stress-dependent manner. *J Cell Mol Med* 2021;25:4466–77.
33 Liu X, Qian L, Nan H, *et al*. Function of the transforming growth factor-B1/C-Jun N-terminal kinase signaling pathway in the action of thalidomide on a rat model of pulmonary fibrosis. *Exp Ther Med* 2014;7:669–74.
34 Ashcroft T, Simpson JM, Timbrell V. Simple method of estimating severity of pulmonary fibrosis on a numerical scale. *J Clin Pathol* 1988;41:467–70.
35 Mei S, Wang S, Jin S, *et al*. Human Adipose tissue-derived stromal cells attenuate the multiple organ injuries induced by sepsis and mechanical ventilation in mice. *Inflammation* 2019;42:485–95.
36 Dhillon AS, Hagan S, Rath O, *et al*. MAP kinase signalling pathways in cancer. *Oncogene* 2007;26:3279–90.
37 Papazian L, Doddoli C, Chetaille B, *et al*. A contributive result of open-lung biopsy improves survival in acute respiratory distress syndrome patients. *Crit Care Med* 2007;35:755–62.
38 Martin C, Papazian L, Payan MJ, *et al*. Pulmonary fibrosis correlates with outcome in adult respiratory distress syndrome. a study in mechanically ventilated patients. *Chest* 1995;107:196–200.
39 Kadota T, Fujita Y, Araya J, *et al*. Human bronchial epithelial cell-derived extracellular Vesicle therapy for pulmonary fibrosis via inhibition of TGF-B-WNT crosstalk. *J Extracell Vesicles* 2021;10:e12124.
40 Kadota T, Yoshioka Y, Fujita Y, *et al*. Extracellular vesicles from fibroblasts induce epithelial-cell senescence in pulmonary fibrosis. *Am J Respir Cell Mol Biol* 2020;63:623–36.
41 Cargnello M, Roux PP. Activation and function of the MAPKs and their substrates, the MAPK-activated protein Kinases. *Microbiol Mol Biol Rev* 2011;75:50–83.
42 Yoshida K, Kuwano K, Hagimoto N, *et al*. MAP kinase activation and apoptosis in lung tissues from patients with idiopathic pulmonary fibrosis. *J Pathol* 2002;198:388–96.
43 Li X, Ye C, Mulati M, *et al*. Ellipticine blocks synergistic effects of IL-17A and TNF-A in epithelial cells and alleviates severe acute pancreatitis-associated acute lung injury. *Biochem Pharmacol* 2020;177:113992.
44 Nie Y, Yu K, Li B, *et al*. S-allyl-L-Cysteine attenuates bleomycin-induced pulmonary fibrosis and inflammation via AKT/NF-KB signaling pathway in mice. *J Pharmacol Sci* 2019;139:377–84.